Modeling of Particles Growth in Styrene Polymerization, Effect of Particle Mass Transfer on Polymerization Behavior and Molecular Weight Distribution

S. R. SULTTAN[1], W J N FERNANDO[1], Z. M. SHAKOOR[2], S.A. SATA[1,*]

[1] *School of Chemical Engineering, Universiti Sains Malaysia, 14300 Nibong Tebal, Penang, Malaysia*
[2] *Chemical Engineering Departments, University of Technology, Baghdad, Iraq*

ABSTRACT: A detailed mathematical model for styrene free radical polymerization system based on the multigrain model (MGM) and polymeric multigrain model (PMGM) has been developed to predict radial monomer concentration within the growing macro particle and particle growth factor, effective parameters on broadening of the molecular weight distribution (MWD), number and weight average of the molecular weight and poly dispersity index (PDI). In this model the more important parameter including time of polymerization, initial size of the initiator particles and diffusion resistance are illustrated through simulation. The validation of the model with experimental data has given a good agreement results and show that the model is able to predict a correct monomer profile, polymerization rate, particle growth factor and more important polymer properties represent by molecular weight and (MWD). The improved algorithm can easily be used to model industrial reactors where additional mass transfer of particles growth effects (physicochemical effects) is present. In addition, the effects of intraparticle and external boundary layer transport resistance on the kinetic behavior and polymer properties are explored.

Keywords: Modeling, Particle growth, Multigrain model, Polystyrene, Mass Transfer.

1.0   INTRODUCTION

Polystyrene is one of the most widely used kinds of plastic; about one million tons of styrene homo polymer are produced annually in the United States [1]. Polystyrene is synthesized via the free-radical polymerization mechanism; the typical application for polystyrene includes food packaging, toys, appliances and compact disc cases. [1].

In spite of extensive research over many years, there is still great controversy about several aspects of the polymerization process ranging from the kinetic mechanisms to the morphology of the growing polymer particles. The kinetic of polymerization is often masked by intraparticle and interfacial mass and heat transfer limitations. The simplest type of model describe this phenomena is based on a spherical initiator or catalyst particle with a spherical shell of polymer deposited around it. Models based on this geometry are commonly called "solid core" models SCM. Monomer diffusion through the polymer shell to active site on the initiator or catalyst surface is the central theme of these models.

Schmeal *et al.* [2-3] and Nagel *et al.* [4], used the solid core model for olefins polymerization using heterogeneous Ziegler-Natta catalysts. It is shown that for a single type of active site, this model could not predict broad MWDs.
Singh *et al.* [5] and Galvan *et al.* [6-7] proposed the polymeric flow model (PFM), this model assumes that growing polymer chains and catalyst fragments form a continuum, diffusion of both reagents and heat takes place through the pseudo-homogeneous polymer matrix.

In the last two decades, more papers have been published on the modeling of polymer particle growth and morphology, mostly based on the multi grain model (MGM) of Floyd *et al.* [8-10], shown schematically in Figure 1. The model structure is based on

*Corresponding author: S.A. Sata, Email: chhairi@eng.usm.my

numerous experimental observations that the original initiator or catalyst particle quickly breaks up into many small fragments which are dispersed throughout the growing polymer. Thus, the large polymer particle (macro particles) is comprised of many small polymer particles (micro particles), which encapsulate these catalyst fragments. All of the micro particles at a given macro particles radius are assumed to be the same size. For monomer to reach the active sites, it must diffuse through the macro pores between micro particles and then through the polymer of the micro particles themselves. In general, the effective diffusion coefficients for two regimes are not equal. We also include the possibility of an equilibrium sorption of monomer at the surface of the micro particle. The disadvantage of this model takes excessive computer time to get results.
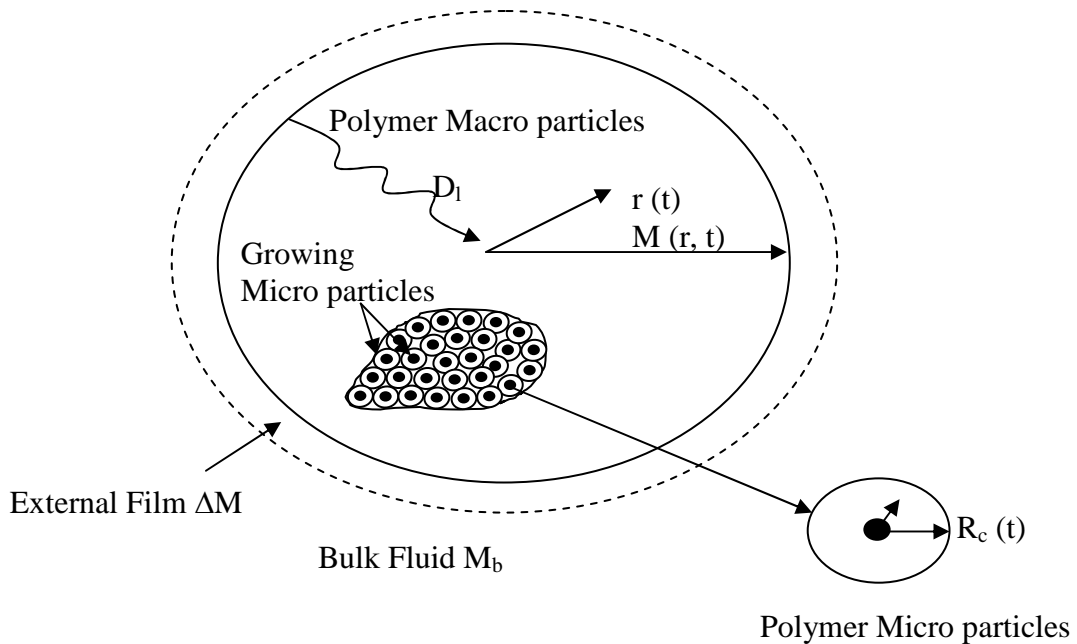

Figure 1: Schematic representation of the Multigrain Model [8]

Sarkar and Gupta [11-12] derived a model called polymeric multigrain model (PMGM) that combines features of the multigrain model with some features of the simplified polymer flow model. The authors observed a significant computational time reduction without significant error increase of results in (PMGM) model. They found that (PMGM) can predict the poly dispersity values higher than that of the multigrain model predictions for single site and deactivating catalysts.

Kanellopoulos *et al.* [13] developed a model called random – pore polymeric flow model RPPFM based on the polymeric flow model (PFM), for gas-phase olefin polymerization accounting for both internal and external mass and heat transfer resistances. It has been shown that both the polymerization rate and particle overheating increase with increasing initial catalyst size and active metal concentration, and also shown the present of a diluent (e.g., nitrogen) in the bulk phase introduces an additional resistance to the monomer transfer from the bulk phase to the active metal sites. And demonstrated that the monomer sorption kinetics greatly affects the polymerization rate and the particle overheating especially during the first few seconds of the polymerization.

Finally, Chen & Liu [14] and Liu [15] presented a modified model for single particle propylene polymerization using heterogeneous Ziegler-Natta catalysts mainly extended from polymeric multigrain model (PMGM) and multigrain model (MGM), by taking the effect of monomer diffusion at both the macro- and micro particle levels, It has been observed that the

model can predict higher values of poly dispersity index (PDI about 6–25) with obtaining some results which are more applicable to the conditions existing in most polymerizations of industrial interest.

It is clearly from the publications above most models applied on the polypropylene polymerization using Ziegler-Natta catalysts in gas and slurry phase. In this paper an appropriate model describing the particles growth in styrene free radical polymerization based on the multigrain model (MGM) and polymeric multigrain model (PMGM) to predicts the polymerization rate and particle growth, effective parameters on broadening of the molecular weight distribution, number and weight average of the molecular weight and poly dispersity index.

2.0   MODELING OF POLYMER PARTICLE

Radial gradients in the growing polymer particle, either of active site or of monomer, create a distributed system in which the local rates of monomer incorporation and chain growth are position dependent, by including a complete kinetic scheme for polymerization in the model. It is possible the predict polymer composition and molecular weight in the growing particle as a function of position and time, this section outlines the development of such a model. The best description model for growing particle shows in Figure 2. As mentioned previous, that the original initiator particle quickly breaks up into many small fragments which are dispersed throughout the growing polymer. Thus, the macro particles are comprised of many micro particles, which encapsulate these initiator fragments.

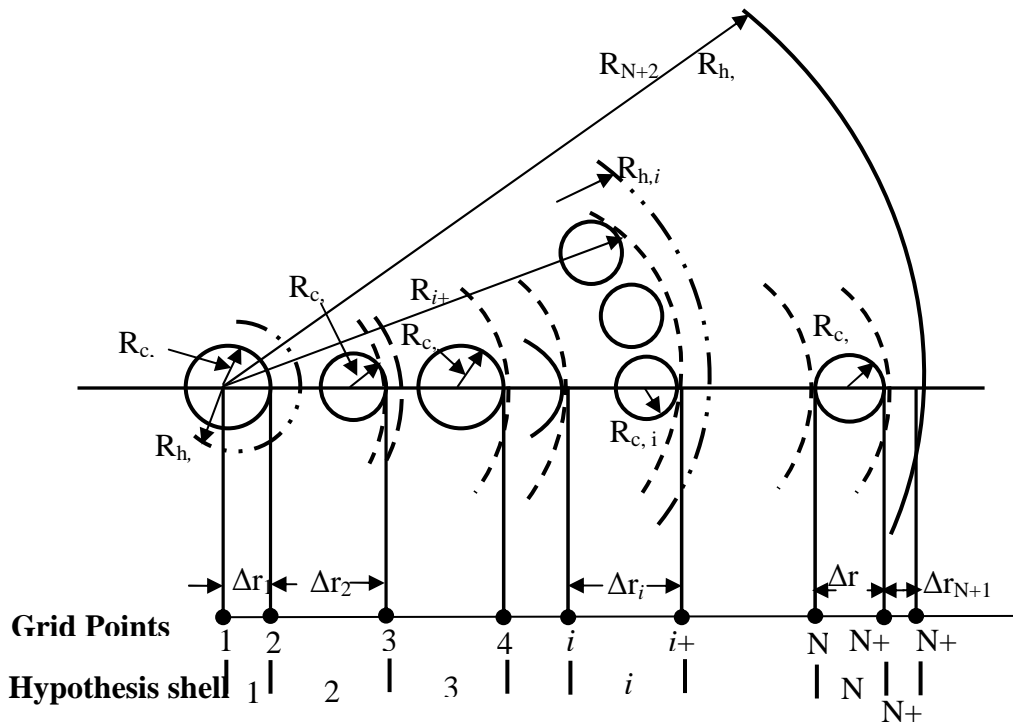**Figure 2:** Schematic of PMGM model. [14]

In Figure 2, we note the hypothesis radius of macro particle shells that define it by (Rh_i) and the micro particle can be placed at the mid-point of each hypothesis shell. At time zero, it is assumed there is no monomer diffusion toward initiator surface so the sizes of all shells are equal. Whenever the polymerization starts, all monomer particles diffuse and

reach to the active site on the initiator surface. In fact, all the micro particles are surrounded by growing polymer chains. Therefore their size, volume and position are change so it is necessary to update all the position and volumes at any time interval.

All of the micro particles at a given macro particles radius are assumed to be the same size and spherical. We consider the macro particle of (N) shell in which every shell has been filled out with (N_i) micro particles, which can be calculated by equations (a & b) in Table 1.

To model the particles growing, relation must be developed between the monomer concentration in the macro and micro particles and the radial shell growth particle yield. The governing equation for the diffusion of monomer in a single spherical macro particle is:

$$\frac{\partial M(r,t)}{\partial t} = \frac{D_{ef}}{r^2} \frac{\partial}{\partial r}\left(r^2 \frac{\partial M}{\partial r}\right) - R_P \tag{1}$$

I. C. $\qquad M(r,0) = M_o \tag{2}$

B. C. 1 $\qquad \dfrac{\partial M(0,t)}{\partial r} = 0 \tag{3}$

B. C. 2 $\qquad D_e \dfrac{\partial M}{\partial r}(R_{N+2},t) = k_1(M_b - M) \tag{4}$

Where (M) is the monomer concentration in the macro particle, (D_{ef}) is the effective diffusively of monomer, (M_0) and (M_b) are the initial and bulk monomer concentration respectively, (k_1) is the mass transfer coefficient in the external film and (R_{pv}) is the reaction rate represents the total rate of consumption of monomer.

In this model, since the initiator fragments are assumed to be in a continuum of polymer also employed by Sarkar and Gupta [11] in (PMGM), there is no macro-particle porosity term in Equation (1), in contrast to that in the multigrain model (MGM) Floyd *et al.* [8-10].

The radial profile of monomer concentration in the micro particle is the same as that for the solid core model:

$$\frac{\partial M_c(r,t)}{\partial t} = \frac{D_s}{r^2} \frac{\partial}{\partial r}\left(r^2 \frac{\partial M_c}{\partial r}\right) \tag{5}$$

I. C. $\qquad M_c(r,0) = M_{co} = 0 \tag{6}$

B. C. 1 $\qquad 4\pi R_c^2 D_s \dfrac{\partial M_c(R_c,t)}{\partial r} = \dfrac{4}{3}\pi R_c^3 R_{pc} \tag{7}$

B. C. 2 $\qquad M_c(r = R_s,t) = M_{eq} = k_e M \leq M \tag{8}$

Where (D_s) is the effective diffusivity of monomer in the micro particle, (M_{eq}) is the equilibrium concentration of monomer in the interface between micro- and macro particles, (M_c) is the monomer concentration in the micro particle, (Mc_0) is the initial monomer

concentration in the micro particle, (R_{pc}) is the rate of polymerization on the surface of initiator fragments, (R_c) is the radius of initiator fragments in the micro particle, r is the radial position in the micro particle, and (R_s) is the radius of the micro particle.

Using the quasi steady state approximation (QSSA) presented in Hutchinson *et al.* [16] (M_c) is easily obtained as:

$$M_c = \frac{k_e M}{1 + \frac{R_c^2}{3D_s}\left(1 - \frac{R_c}{R_s}\right)k_p C^*}$$

(9)

Where (M_c) is the monomer concentration at the initiator surface in the micro particle. (ke) represents the corresponding equilibrium constant for monomer absorption in the micro particle.

Equation (1) is converted to a set of (N+2) ordinary differential equations (ODEs) of monomer concentration at (*i*) position by using a finite difference technique that was stated by Finlayson [17], with regard to the unequally spaced grid points as shown in Figure 2. These equations are list in Table 1. In these, subscript *i* (*i* = 1, 2…..N+2), on any variable, indicates its value at the *i*th grid point. The calculations of (Δr and R) at (*ith*) position are given in Appendix 1. The radius, ($R_{c,i}$) of the catalyst subparticle in the(*ith*) shell, are generated randomly using the equations of Nagel *et al.*[4]

Table 1: Equation for N_i and M_i for the (PGM)

$N_1 = 1$	(a)
$N_i = \dfrac{6(1-\varepsilon)\left[R_{s,i} + 2\sum_{j=2}^{i-1} R_{s,j} + R_{s,i}\right]^2}{R_{s,i}^2} \qquad i = 2,3,\ldots,N$	(b)
$\dfrac{dM_1}{dt}\dfrac{2D_{e,1}(M_2 - M_1)}{(\Delta r_1)^2} - R_{p,1}$	(c)
$\dfrac{dM_i}{dt} = \dfrac{2D_{e,i}}{\Delta r_i + \Delta r_{i-1}}\left[M_{i+1}\left(\dfrac{1}{\Delta r_i} + \dfrac{1}{R_i}\right) - M_i\left(\dfrac{1}{\Delta r_i} + \dfrac{1}{\Delta r_{i-1}}\right) + M_{i-1}\left(\dfrac{1}{\Delta r_{i-1}} - \dfrac{1}{R_i}\right)\right]$ $\qquad - R_{p,i} \qquad\qquad i = 2,3 \ldots\ldots\ldots, N+1$	(d)
$\dfrac{dM_{N+2}}{dt} = -M_{N+2}\left[\dfrac{2k_1}{\Delta r_{N+1}} + \dfrac{2D_{e,N+2}}{(\Delta r_{N+1})^2} + \dfrac{2k_1}{R_{N+2}}\right] + M_{N+1}\left[\dfrac{2D_{e,N+2}}{(\Delta r_{N+1})^2}\right] + M_b\left[\dfrac{2k_1}{\Delta r_{N+1}} + \dfrac{2k_1}{R_{N+2}}\right]$ $\qquad - R_{p,N+2}$	(e)

The effective diffusivity, (D_{ef}) is commonly estimated from the diffusivity of the component in the bulk phase of the reactor (D_1), using the expression below:

$$D_{ef} = D_1 \cdot \frac{\varepsilon}{\tau}$$

(10)

Where (ε) and (τ) are the porosity and tortuosity of the macro particle, respectively. Sarkar & Gupta [11] corrected the diffusivity by a factor proportional to the amount of polymer in the particles, the correction factor equal to the area-fraction of polymer (assumed to be the same as its volume fraction) in the macro particle at any radial location. Thus, as the particle fills up with polymer, the effective diffusivity decreases as follows:

$$D_{e,1} = D_{e,N+2} = D_1 \tag{11}$$

$$D_{e,i+1} = \frac{D_1 N_i R_{s,i}^3}{(R_{h,i}^3 - R_{h,i-1}^3)}; \quad i = 2,3, \ldots \ldots \ldots, N \tag{12}$$

Where (D_1) is the diffusion of monomer through pure polymer. So the effective diffusion coeffiecient here is considered to be change any time during particle growth in opposition to Floyd *et al.*[8-10]

The net rate of consumption of monomer per unit macroscopic volume at any radial location, (R_{pv}), can be calculated by:

$$R_{p,1} = R_{p,N+2} = 0 \tag{13}$$

$$R_{p,i} = \frac{\left(\frac{4\pi}{3}\right)(3600)k_p\lambda_o M_i N_{i-1}\left(R_{s,i-1}\right)^3}{\left(\frac{4\pi}{3}\right)\left(R_{h,i}^3 - R_{h,i-1}^3\right)}; \quad i = 2,3, \ldots \ldots \ldots \ldots, N+1 \tag{14}$$

So the corresponding overall time-dependent reaction rate can be calculated:

$$R_{overall} = \frac{k_p\lambda_o \sum_{i=1}^{N}(N_i M_{c,i})}{\rho_p \sum_{i=1}^{N} N_i} \tag{15}$$

The monomer concentration in the micro particle at any radial position is given by:

$$M_{c,i} = \frac{k_e M_i}{1 + \frac{R_c^2}{3D_s}\left(1 - \frac{R_c}{R_{s,i}}\right)k_p\lambda_o} \tag{16}$$

Where k_p (t) is the constant propagation rate and λo (t) is the active sites concentration on the surface of the micro particle, which can be calculated from the kinetic reaction model as shown in Table 2.

Table 2: Kinetic reactions scheme of styrene polymerization

Initiation	$R^{\cdot} + M_c \xrightarrow{k_i} R_1^{\cdot}$
Propagation	$R_n^{\cdot} + M_c \xrightarrow{k_p} R_{n+1}^{\cdot}$
Termination	$R_n^{\cdot} + R_m^{\cdot} \xrightarrow{k_{tc}} P_{n+m}$

According to the kinetic reactions in Table 2, a large set of non-linear ordinary differential equations is derived to describe the mass conservation of the various reactants in a well stirred batch polymerization reactor as shown in equations below:-
For Initiator decomposition:

$$\frac{d(I)}{dt} = -k_d I \tag{17}$$

For Free Radical species:

$$\frac{d(R_1^{\cdot})}{dt} = 2fk_d I - k_p M_c R_1^{\cdot} - k_t R_1 \sum_{i=1}^{\infty} R_i^{\cdot} + k_m M_c \sum_{i=2}^{\infty} R_i^{\cdot} \tag{18}$$

$$\frac{d(R_n^{\cdot})}{dt} = k_p M_c (R_{n-1}^{\cdot} - R_n^{\cdot}) - k_m M_c R_n^{\cdot} - k_t R_n^{\cdot} \sum_{m=1}^{\infty} R_m^{\cdot} \tag{19}$$

For the monomer species:

$$\frac{dM}{dt} = -k_p M_c \sum_{i}^{\infty} R_i^{\cdot} - k_m M_c \sum_{i}^{\infty} R_i^{\cdot} \tag{20}$$

For the dead polymer species:

$$\frac{d(P_n)}{dt} = k_m M_c R_n^{\cdot} + k_{td} R_n^{\cdot} \sum_{m=1}^{\infty} R_m^{\cdot} + (\frac{k_{tc}}{2}) \sum_{m=1}^{n=1} R_m^{\cdot} R_{n-m}^{\cdot} \tag{21}$$

In derivation equations above, the following assumptions were made to simplify the mathematical descriptions:
1. Quasi-steady-state approximation (QSSA) for live radicals and dead polymer concentration.
2. All the reaction steps are irreversible.
3. The rate of chain transfer to solvent reactions is negligible.
4. There is no change in volume.
5. Perfect mixing and constant reacting heat capacity and density exist.

Equations in Table 2 represent an infinite number of differential equations since (n) can vary from (2) to infinity. Therefore, a rigorous solution requires roughly (10000-50000) stiff differential equations to be solved simultaneously. This large number of equations can be

reduced to set of fewer non-linear differential equations by method of moments. In this method, the (kth) moment of the live radical and the dead polymer concentration are defined as:

$$\lambda_k = \sum_{i=1}^{\infty} i^k R_i \tag{22}$$

$$\mu_k = \sum_{i=1}^{\infty} i^k P_i \tag{23}$$

Where (λ_o) represents the total concentration of live radicals and (μ_o) denotes the total dead polymer concentration. To eliminate the stiff condition of the equations, quasi-steady-state assumption was made to reduce the number of equations. The quasi-steady-state assumes that the rate of change of radical concentration is almost zero. Then the final simplified mathematical model equations shown below:

$$\frac{d(I)}{dt} = -k_d I \tag{24}$$

$$\frac{d\lambda_o}{dt} = 2fk_d I - k_t \lambda_o^2 \tag{25}$$

$$\frac{dM}{dt} = -k_p M_c \lambda_o \tag{26}$$

$$\frac{d\lambda_1}{dt} = 2fk_d I + k_p M_c \lambda_o - k_t \lambda_o \lambda_1 \tag{27}$$

$$\frac{d\lambda_2}{dt} = 2fk_d I M_c + k_p M_c (\lambda_o + 2\lambda_1) - k_t \lambda_o \lambda_2 \tag{28}$$

$$\frac{d\mu_o}{dt} = 2fk_d I \tag{29}$$

$$\frac{d\mu_1}{dt} = k_t \lambda_o \lambda_1 \tag{30}$$

$$\frac{d\mu_2}{dt} = k_t \lambda_o \lambda_2 \tag{31}$$

Number average (M_n) and weight average molecular weights (M_w) of the polymer can be calculated from the moment's (λ_k) and (μ_k) of the (MWD). The number average chain length is the ratio of the first moment to the zeros moment of (MWD) and the weight average chain length is the ratio of the second moment to the first moment of (MWD). The number average (M_n) and weight average (M_w) molecular weights of the polymer are obtained by multiplying theses chain lengths with the molecular weight of unit monomer (MW).

$$M_n = MW \left[\frac{\lambda_1 + \mu_1}{\lambda_o + \mu_o} \right] \tag{32}$$

$$M_w = MW \left[\frac{\lambda_2 + \mu_2}{\lambda_1 + \mu_1} \right] \tag{33}$$

And the poly dispersity index (PID) is given by:

$$PDI = \frac{M_w}{M_n} = \frac{(\lambda_2 + \mu_2)(\lambda_o + \mu_o)}{(\lambda_1 + \mu_1)^2} \tag{34}$$

The number and weight average molecular weights and (PDI) of the polymer in the (*i*th) shell are obtained using:

$$M_{n,i} = MW \left[\frac{\lambda_1 + \mu_1}{\lambda_o + \mu_o}\right]_i \tag{35}$$

$$M_{w,i} = MW \left[\frac{\lambda_2 + \mu_2}{\lambda_1 + \mu_1}\right]_i \tag{35}$$

$$PDI_i = \frac{M_{wi}}{M_{ni}} \qquad\qquad i = 1,2,\ldots\ldots N+1 \tag{37}$$

This model was implemented by using Matlab M - Function program and solved with a sub routine called ODE15S which is usually used for stiff differential equations. In Table 3, the details of the algorithm of computer simulation program are presented for all the related equations used in this model.

Table 3: algorithm of computer simulation program

```
                    ┌─────────┐
                    │  Start  │
                    └─────────┘
                         │
                         ▼
    ┌───────────────────────────────────────────────┐
    │  Read N, kd, kp, kt, I_o, D_1, M_o, k_1, Δt    │
    └───────────────────────────────────────────────┘
                         │
                         ▼
    ┌───────────────────────────────────────────────┐
    │  Set t=0, Input initial condition Generate Rc, │
    │       calculate R_i, R_hi and Δr_i             │
    └───────────────────────────────────────────────┘
                         │
                         ▼
    ┌───────────────────────────────────────────────┐
    │ Compute coefficients of the finite difference  │
    │            N+2 ODEs and D_ef                   │◄──┐
    └───────────────────────────────────────────────┘   │
                         │                               │
                         ▼                               │
    ┌───────────────────────────────────────────────┐   │
    │      Call ODE15s to solve N+2 ODEs             │   │
    │   To compute monomer profile at t+Δt           │   │
    └───────────────────────────────────────────────┘   │
                         │                               │
                         ▼                               │
    ┌───────────────────────────────────────────────┐   │
    │    Updating the volume of macro particle       │   │
    │        update R_i, R_hi and Δr_i               │   │
    └───────────────────────────────────────────────┘   │
                         │                               │
                         ▼                               │
    ┌───────────────────────────────────────────────┐   │
    │        Call ODE15s for moment                  │   │
    │          equations at t+Δt                     │   │
    └───────────────────────────────────────────────┘   │
                         │                               │
                         ▼                               │
    ┌───────────────────────────────────────────────┐   │
    │         Calculate Mn, Mw and PDI               │   │
    └───────────────────────────────────────────────┘   │
                         │                               │
                         ▼                               │
                    ╱──────────╲                         │
                  ╱  t ≤ t_reaction ╲──────────────────┘
                    ╲──────────╱
                         │
                         ▼
              ┌─────────────────────┐
              │   Save required     │
              │      results        │
              └─────────────────────┘
                         │
                         ▼
                    ┌─────────┐
                    │   End   │
                    └─────────┘
```
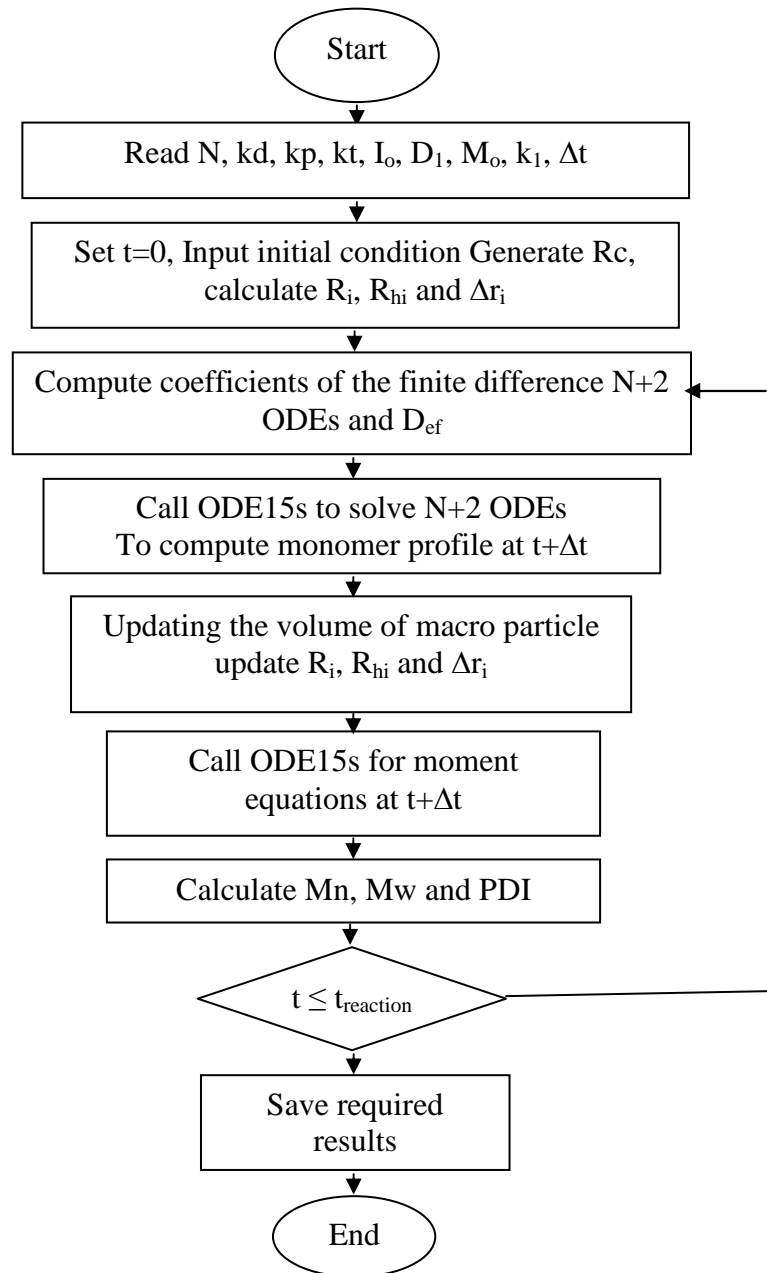
3.0   RESULTS AND DISCUSSION

The results obtained from this model can be divided in two sections, the first section study the mass transfer effects on the monomer concentration within the growing macro particle and the second section study the behavior of the molecular weight and molecular weight distribution (MWD) during styrene polymerization.

3.1   Mass Transfer Effects on Polymerization Kinetics

In this section the results are general using the present model to study the effects of various parameters such as time of polymerization, diffusion resistance (represented by D_1),

and initiator particle size (R_c) on the monomer concentration within the growing macro particle. The set of realistic values of kinetic and physical parameter taken from experimental studies are presented in Table 4.

Table 4: Reference values of parameters for simulation of styrene polymerization [18]

Parameter	Value	Unit
M_o	7.28	mol .dm^{-3}
I_o	0.052	mol .dm^{-3}
R_c	1	µm
R_o	20	µm
D_1	$1*10^{-12}$	m^2.s^{-1}
D_s	$1*10^{-11}$	m^2.s^{-1}
R	1.987	Cal.mol^{-1} K^{-1}
T	363	K
MW	104.14	gm.mol^{-1}
kd	$6.38*10^{13}$ exp(-29700/RT)	s^{-1}
kp	$1*10^{7.63}$ exp(-7740/RT)	dm^3. mol^{-1} .s^{-1}
kt	$1.255*10^9$ exp(-1675/RT)	dm^3. mol^{-1} .s^{-1}

Figure 3 shows profiles of the monomer concentration as a function of radial position within the growing macro particle at different reaction times. From this figure it is clearly seen that significant monomer concentration gradients exist across the particle radius in the early stages of the reaction; this comes about because in the initial stages of polymerization the rate of reaction is at maximum and the surface area exposed to the monomer source is at a minimum, the effects of intraparticle mass transfer will be most pronounced for large particle of initiator and high activities, besides the intraparticle mass transfer resistance in the pores of growing polymer particle. While the former will decrease with time as the reaction rate decreases, the latter will increase slightly with time as the polymer film surrounding the active sites becomes thicker.
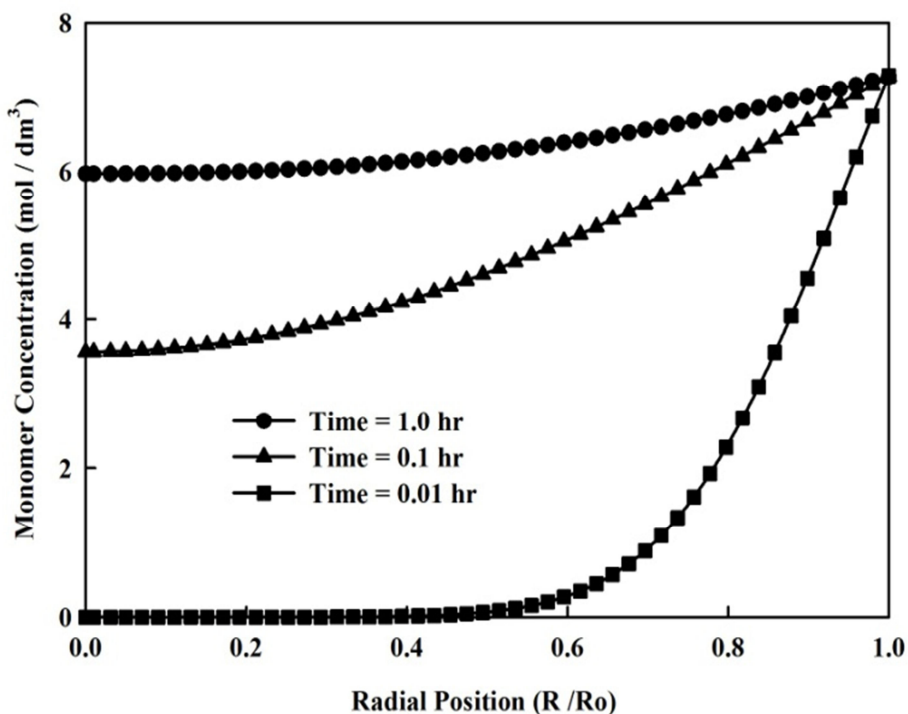

Figure 3: Profiles of the monomer concentration as a function of radial position within the growing macro particle at R_c = 1µm, D_1=$1*10^{-13}$ and different reaction times.

The behavior of the monomer concentration as a function of radial position within the growing macro particle at varying initiator particle size (R_c) illustrated in Figure 4, from this figure it is pronounced the increased initiator particle size lead to decreasing monomer concentration within the growing macro particle; because of increased initiator particle size results in a large increase in monomer consumption rate.
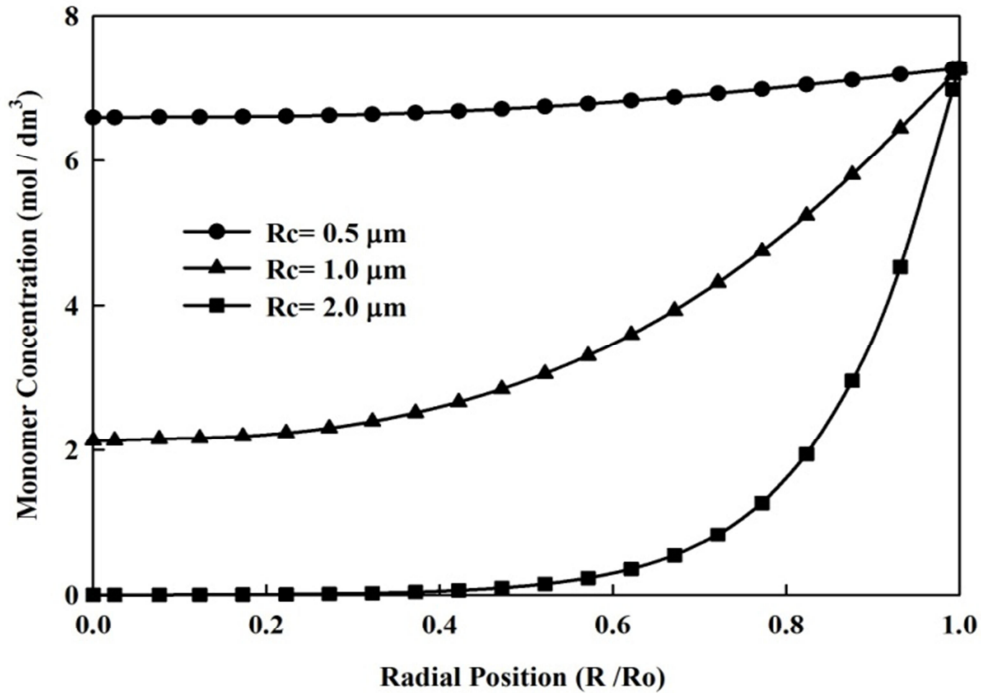

Figure 4: Monomer concentration as a function of radial position within the growing macro particle at time = 2 hr, $D_1 = 1*10^{-13}$ and different initiator particle.

Figure 5 shows how the diffusion resistance effects on macro particle monomer concentration, which is determined by the large particle diffusivity (D_1), as seen from this figure the acceleration behavior becomes more pronounced as the diffusivity decreases and diffusion resistance becomes more severe. One major conclusion from that analysis was that mass transfer resistance is most severe early in the polymerization and decreases as the polymer particle grows in size.
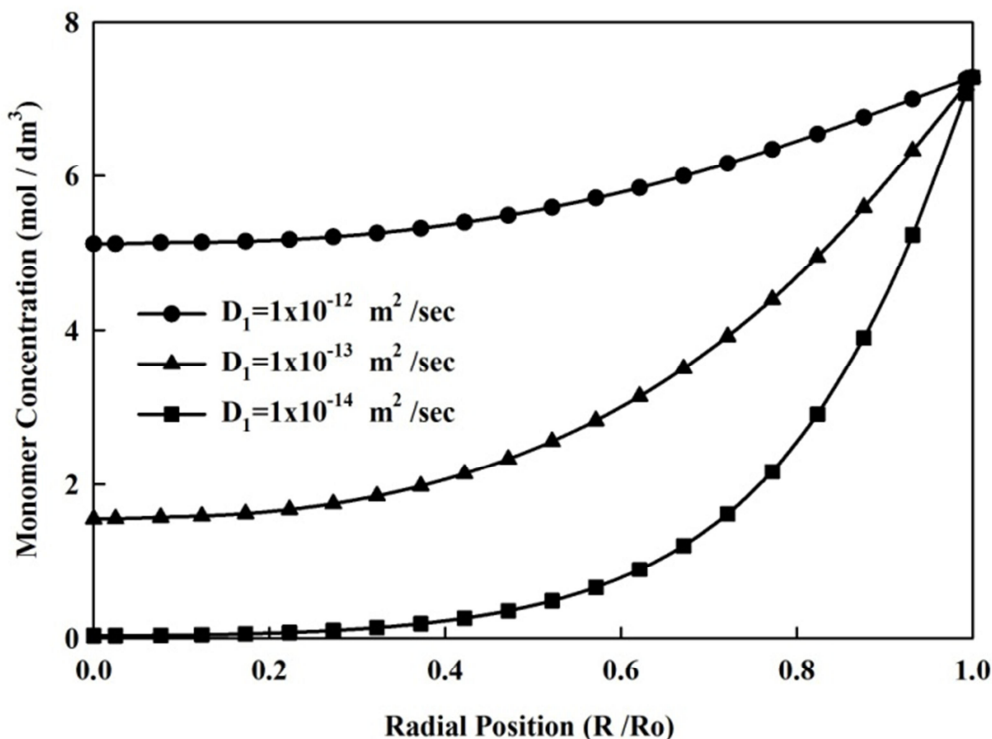
Figure 5: Monomer concentration as a function of radial position within the growing macro particle at time = 2 hr, R_c = 1μm, and different degree of diffusion resistance (D_1).

3.2   Molecular Weight and Molecular Weight Distribution

In this section, the behavior of the molecular weight and molecular weight distribution (MWD) during styrene polymerization will be considered. As discussed previously, the number and weight average molecular weight and the poly dispersity index may be obtained from ratios between the zeros, first and second moments. Results predicted from this model have been validated with data obtained from a laboratory batch polymerization reactor of Vicevic *et al.* [18].

Figures 6 & 7 shows the simulated results obtained by our model and experimental work of Vicevic *et al.* [18] for number average (Mn) and weight average (Mw) molecular weight as a function of time. As commonly observed in many other addition polymerization processes, both the number average (Mn) and weight average (Mw) molecular weight values increase rapidly in short reaction time at the beginning of polymerization and then slightly decrease with time. The model gives a good agreement with experimental results within a confidence interval of ± 5%.

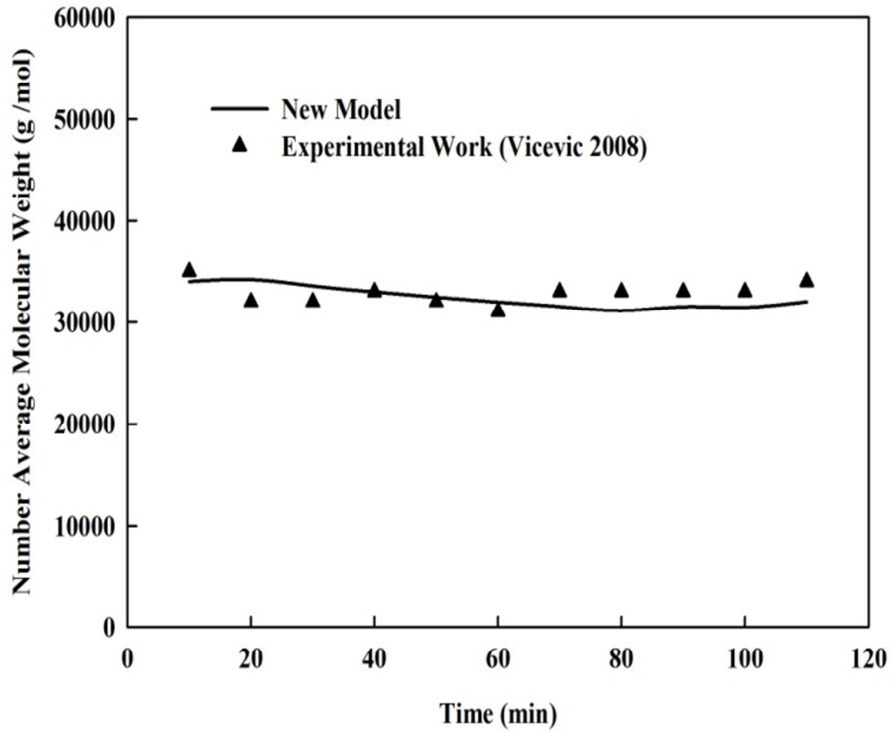**Figure 6:** Number average molecular weight predicted by model and experimental work (Vicevic 2008) as a function of time at R_c = 1μm, D_1=1*10^{-13}.
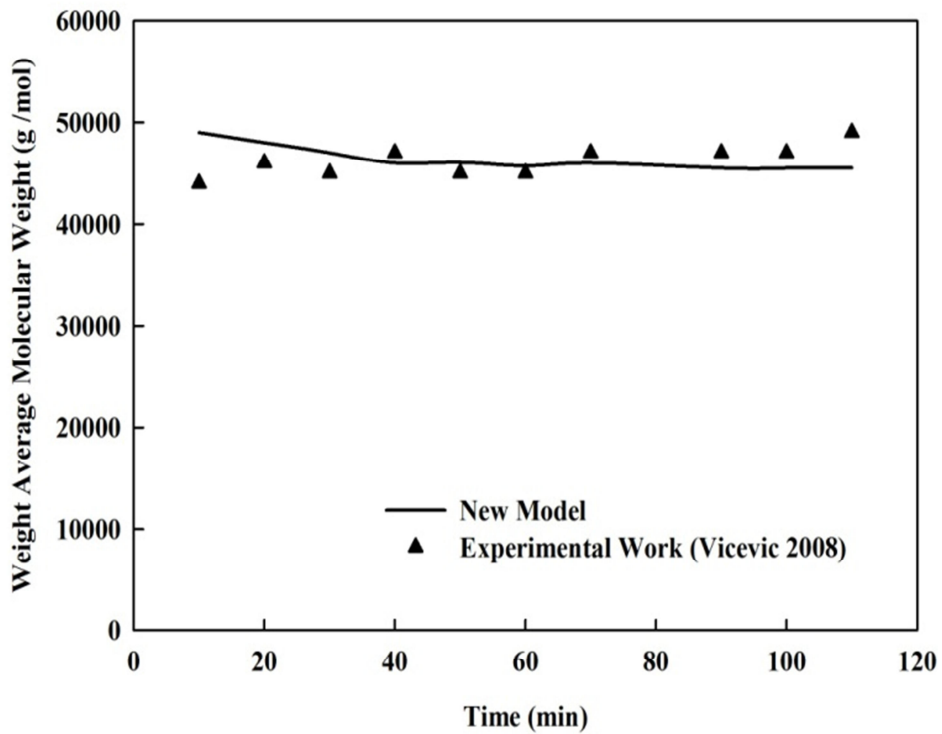

Figure 7: Weight average molecular weight predicted by model and experimental work (Vicevic 2008) as a function of time at R_c = 1μm, D_1=1*10^{-13}.

The results of polydispersity index, (PDI) as a function of polymerization time can be seen in Figure 8, these results are in a good agreement with (PDI) present in the literature for the styrene polymerization in a batch reactor.
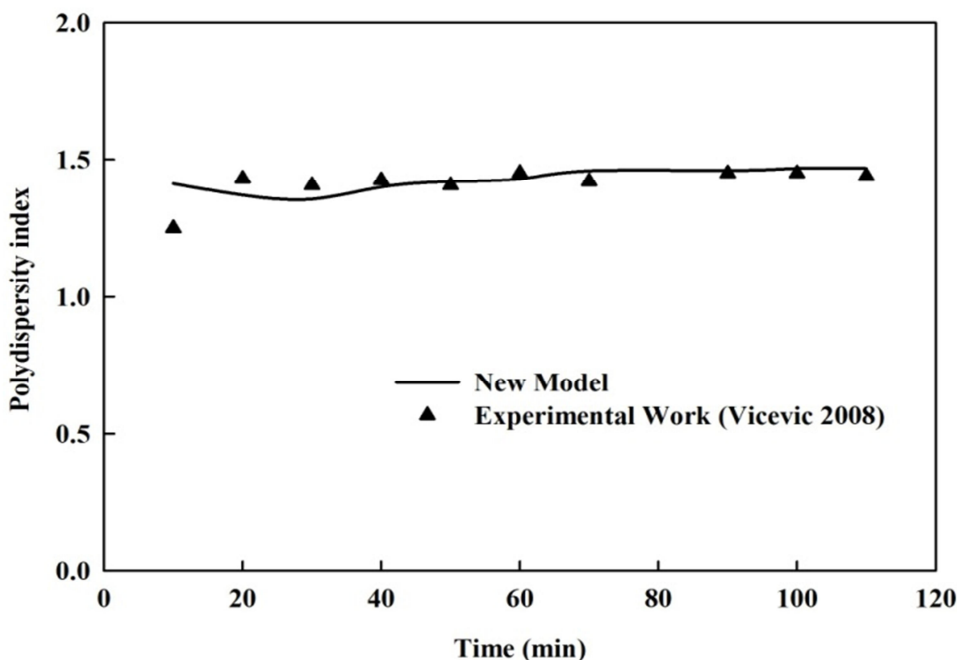

Figure 8: Polydispersity index predicted by model and experimental work (Vicevic 2008) as a function of time at R_c = 1µm, D_1=1*10^{-13}

4.0 CONCLUSIONS

A comprehensive mathematical model based on multigrain model (MGM) and polymeric multigrain model (PMGM), has been present and used for simulation of styrene free radical polymerization process, which can be also used for other different polymers, validation of the model with experimental data show that this model is able to predict a correct monomer profile, polymerization rate, particle growth factor and more important polymer properties represent by molecular weight and molecular weight distribution (MWD). The improved algorithm can easily be used to model industrial reactors where additional physicochemical effects are present.

5.0 ACKNOWLEDGMENTS

6.0 REFERENCES

[1]   G. G. Odian, *Principles of polymerization*. Hoboken, N.J.: Wiley-Interscience, 2004.

[2]   W. R. Schmeal and J. R. Street, "Polymerization in expanding catalyst particles," *AIChE Journal,* vol. 17, pp. 1188-1197, 1971.

[3]   W. R. Schmeal and J. R. Street, "Polymerization in catalyst particles: Calculation of molecular weight distribution," *Journal of Polymer Science: Polymer Physics Edition,* vol. 10, pp. 2173-2187, 1972.

[4]   E. J. Nagel*, et al.*, "Prediction of Molecular Weight Distributions for High-Density Polyolefins," *Industrial & Engineering Chemistry Product Research and Development,* vol. 19, pp. 372-379, 1980.

[5]   D. Singh and R. P. Merrill, "Molecular Weight Distribution of Polyethylene Produced by Ziegler-Natta Catalysts," *Macromolecules,* vol. 4, pp. 599-604, 1971.

[6]   R. Galvan and M. Tirrell, "Orthogonal collocation applied to analysis of heterogeneous Ziegler-Natta polymerization," *Computers & Chemical Engineering,* vol. 10, pp. 77-85, 1986.

[7]   R. Galvan and M. Tirrell, "Molecular weight distribution predictions for heterogeneous Ziegler-Natta polymerization using a two-site model," *Chemical Engineering Science,* vol. 41, pp. 2385-2393, 1986.

[8]   S. Floyd*, et al.*, "Polymerization of olefins through heterogeneous catalysis. III. Polymer particle modelling with an analysis of intraparticle heat and mass transfer effects," *Journal of Applied Polymer Science,* vol. 32, pp. 2935-2960, 1986.

[9]   S. Floyd*, et al.*, "Polymerization of olefines through heterogeneous catalysis IV. Modeling of heat and mass transfer resistance in the polymer particle boundary layer," *Journal of Applied Polymer Science,* vol. 31, pp. 2231-2265, 1986.

[10]   S. Floyd*, et al.*, "Polymerization of olefins through heterogeneous catalysis—V. Gas-liquid mass transfer limitations in liquid slurry reactors," *Journal of Applied Polymer Science,* vol. 32, pp. 5451-5479, 1986.

[11]   P. Sarkar and S. K. Gupta, "Modelling of propylene polymerization in an isothermal slurry reactor," *Polymer,* vol. 32, pp. 2842-2852, 1991.

[12]   P. Sarkar and S. K. Gupta, "Simulation of propylene polymerization: an efficient algorithm," *Polymer,* vol. 33, pp. 1477-1485, 1992.

[13]   V. Kanellopoulos*, et al.*, "Comprehensive Analysis of Single-Particle Growth in Heterogeneous Olefin Polymerization: The Random-Pore Polymeric Flow Model," *Industrial & Engineering Chemistry Research,* vol. 43, pp. 5166-5180, 2004.

[14]   Y. Chen and X. Liu, "Modeling mass transport of propylene polymerization on Ziegler-Natta catalyst," *Polymer,* vol. 46, pp. 9434-9442, 2005.

[15]   X. Liu, "Modeling and Simulation of Heterogeneous Catalyzed Propylene Polymerization," *Chinese Journal of Chemical Engineering,* vol. 15, pp. 545-553, 2007.

[16]   R. A. Hutchinson*, et al.*, "Polymerization of olefins through heterogeneous catalysis X: Modeling of particle growth and morphology," *Journal of Applied Polymer Science,* vol. 44, pp. 1389-1414, 1992.

[17]   B. A. Finlayson, *Nonlinear analysis in chemical engineering*: McGraw-Hill International Book Co., 1980.

[18]   M. Vicevic*, et al.*, "Kinetics of styrene free radical polymerisation in the spinning disc reactor," *Chemical Engineering Journal,* vol. 135, pp. 78-82, 2008.

Glossary/Nomenclature

$D_{ef,I}$	Effective macroparticle diffusivity, at the *i*th grid point ($m^2.s^{-1}$)
D_1	Monomer diffusivity in pure polymer ($m^2.s^{-1}$)
D_s	Effective microparticle diffusion coefficient ($m^2.s^{-1}$)
k_p	Propagation rate constant ($dm^3.(mol.s)^{-1}$)
k_d	Initiator decomposition rate constant (s^{-1})
k_{tc}	Termination rate constant ($dm^3.(mol.s)^{-1}$)
k_1	liquid film mass transfer coefficient ($m^2.s^{-1}$)
I_o	Initiator initial concentration ($mol.dm^{-3}$)
M_i	Monomer concentration in the macroparticle, at the *i*th grid point ($mol.dm^{-3}$)
M_b	Bulk monomer concentration ($mol.dm^{-3}$)
M_o	Initial monomer concentration ($mol.dm^{-3}$)
$Mc_{,I}$	Monomer concentration at the initiator surface in the microparticle, at the *i*th grid point
M_n	Number average molecular weight
M_w	Weight average molecular weight
MW	Molecular weight of monomer ($g.mol^{-1}$)
N	Number of shell
PDI	Polydispersity index
R	Radial position at the macroparticle level (m)
r_s	Radial position at the microparticle level (m)
R	Universal gas constant ($cal (mol.k)^{-1}$)
R_c	Radius of initiator subparticles (m)
R_{N+2}	Macroparticle radius (m)
R_o	Initial particle radius (m)
$R_{h,i}$	Radius of ith hypothetical shells
$R_{s,I}$	Radius of microparticle at ith hypothetical shells
$R_{pv,I}$	Rate of reaction per unit volume at the ith grid point ($mol (m^3.s)^{-1}$)
$V_{cs,i}$	Volume of the *i*th hypothesis shell
$V_{cc,i}$	Volume of initiator in shell *i*
E	Void fraction of closed packed spheres (= 0.4)
λ_k	Moment of live polymer
λ_o	Total concentration of live radicals

APPENDIX 1

The changes in the shells volume, (ΔV_i) and the location of the grid points (R_i) with time are given in this section. As shown in Figure 2. The hypothetical shell can be defined as ($R_{h,i-1} \le r \le R_{h,i}$) such that the entire polymer produced by the catalyst particles of radius (R_c) are accommodated in it . In the interval (t to t+Δt), the total volume of polymer (V_i) and the volume of microparticle ($V_{s,i}$) produced at ith shell are given by:

$$\frac{dV_i}{dt} = \frac{0.001 k_p \lambda_o M_{c,i} \left(N_i \frac{4\pi}{3} R_{s,i}^3 \right)(MW)}{\rho_p} \tag{1.1}$$

$$\frac{dV_{s,i}}{dt} = \frac{0.001 k_p \lambda_o M_{c,i} \left(\frac{4\pi}{3} R_c^3 \right)(MW)}{\rho_p} \qquad\qquad i = 1,2, \dots \dots \dots N \tag{1.2}$$

With V_i (t=0) and $V_{s,i}$ (t=0) being the initial total volume and volume of every polymer micro particle of ith volume respectively.

$$V_i(t = 0) = \frac{N_i \left(\frac{4\pi}{3} R_c^3 \right)}{(1 - \varepsilon)} \qquad\qquad i = 1,2, \dots \dots \dots N \tag{1.3}$$

$$V_{s,i}(t = 0) = \frac{4\pi}{3} R_c^3 \tag{1.4}$$

We can now define the hypothetical shells at any time by.

$$R_{h,i} = \left(\frac{3}{4\pi} \sum_{j=1}^{i} V_j \right)^{1/3} \qquad\qquad i = 1,2, \dots \dots \dots, N \tag{1.5}$$

Where $R_{h,o} = 0$ and the radius of microparticle at ith shell being:

$$R_{s,i} = \left(\frac{3}{4\pi} V_{s,i} \right)^{1/3} \tag{1.6}$$

The catalyst particles are assumed to be placed at the mid points of each hypothetical shell. Thus:

$$R_{1,i} = R_{h.i-1} + \left(\frac{1}{2} \right) \left(R_{h,i} - R_{h,i-1} \right); \qquad\qquad i = 2,3 \dots \dots N \tag{1.7}$$

Then the computational grid points are related to ($R_{1,i}$) by:

$$R_1 = 0 \tag{1.8}$$
$$R_2 = R_c \tag{1.9}$$
$$R_{i+1} = R_{1,i} + R_{s,i} \qquad\qquad i = 2,3, \dots \dots N \tag{1.10}$$
$$R_{N+2} = R_{h,N} \tag{1.11}$$

The values of (Δr_i) to be used in the equation of Table 1 are given by:

$$\Delta r_i = R_{i+1} - R_i \qquad\qquad i = 1,2, \dots \dots N + 1 \tag{1.12}$$